Rapid quenching of melts in the system La_2O_3–WO_3

Rapid quenching of oxide melts, including oxide mixtures, forms glass (non-crystalline), metastable crystalline or expanded solid solution phases. Sarjeant and Roy [1] obtained a glass of WO_3 as well as its high-temperature phase, and Topol *et al.* [2] later reported no glass formation in WO_3. They surprisingly observed glass formation in pure La_2O_3, but poor glass formation in mixtures with CaO, SiO_2, or both. Glass phases have been obtained in the binary systems between La_2O_3 and TiO_2 [3], Nb_2O_5 [3], Fe_2O_3 [3], Al_2O_3 [4, 5], or Ga_2O_3 [5]. Glass formation in the system La_2O_3–WO_3 is fully expected because WO_3 is one of the glass-forming oxides and La_2O_3 is a modifier oxide, but has not yet been observed. Rapid quenching leads to the formation of the high-temperature phase of $La_2O_3 \cdot 3WO_3$ [6] and $La_2O_3 \cdot 2WO_3$ [7]. This communication describes the complete results of rapid quenching and glass formation in the system La_2O_3–WO_3.

A hammer-and-anvil method employed in a solar furnace was used [5, 8]. A molten globule struck with a hammer, splashes out of the impact area against a water-cooled support and forms thin lamellae 20 to 30 μm thick. The cooling rate of the lamellae was estimated to be 10^5 ° C sec^{-1} [9, 10]. The portion of sample aiming between the hammer and anvil typically forms plates 250 to 500 μm thick. The cooling rate of these plates would be between that of lamellae and that of a fused globule. The globules fused in the centre of the furnace were quickly removed and allowed to cool on the water-cooled support, with a rate estimated to be about 10^2 ° C sec^{-1} [6]. The three types sample obtained were examined by powder X-ray analysis and microscopic observation.

The results summarized in Table I are consistent with previous work except for [2]. They essentially indicate (a) glass formation near the eutectic composition (Fig. 1), (b) high-temperature phases for WO_3, $La_2O_3 \cdot 2WO_3$, $La_2O_3 \cdot WO_3$, and $3La_2O_3 \cdot WO_3$, and (c) low-temperature phases for $3La_2O_3 \cdot 2WO_3$, $7La_2O_3 \cdot 8WO_3$, and La_2O_3. With decreasing cooling rates, the phases tend to form in the direction (A) → (B) → (C). Fused products were almost identical with the low-temperature equilibrium phases except for $3La_2O_3 \cdot 2WO_3$ and $7La_2O_3 \cdot 8WO_3$. The former decomposed to $5La_2O_3 \cdot 2WO_3$ phase by precipi-

TABLE I Results of rapid quenching of melts in the system La_2O_3–WO_3

Composition La_2O_3:WO_3	Phases presented		
	Thin lamellae	Thick lamellae or plates	Globule
100:0	A	A	A
95:5	A + 3:1	–	A + 3:1
90:10	A + 3:1	A + 3:1	A + 3:1
85:15	A	–	A + 3:1
80:20	3:1 + A	3:1 + A	3:1 + A
75:25	3:1	3:1	3:1
73:27	3:1	3:1	3:1
71.4:28.6	3:1 + trace 3:2	3:1	3:1 + trace 3:2
70:30	3:1 + 3:2	3:1 + 3:2	3:1 + 3:2
60:40	3:2	3:2	3:2
50:50	H – 1:1	H – 1:1 + L – 1:1 + trace 7:8	L – 1:1 + trace 7:8
46.8:53.2	H – 1:1	H – 1:1 + trace 7:8	L – 1:1 + 7:8
44.56	H – 1:1 + 7:8 + trace H – 1:2	–	L – 1:1 + 7:8 + L – 1:2
33.3:66.7	H – 1:2	L – 1:2	L – 1:2
25:75	Glass	1:3	1:3
18.2:81.8	Glass	1:4.4	1:4.4
10:90	Glass + H – W	Glass + H – W	1:4.4 + L – W
5:95	Glass + H – W	H – W + L – W	L – W + 1:4.4
0:100	H – W + glass (?)	–	L – W

A = A-type La_2O_3, 3:1 = $3La_2O_3 \cdot WO_3$ solid solution, 3:2 = $3La_2O_3 \cdot 2WO_3$, 1:1 = $La_2O_3 \cdot WO_3$, 7:8 = $2La_2O_3 \cdot 8WO_3$, 1:2 = $La_2O_3 \cdot 2WO_3$, 1:3 = $La_2O_3 \cdot 3WO_3$ (= $La_2(WO_4)_3$), 1:4.4 = $La_{10}W_{22}O_{81}$, W = WO_3, H = high-temperature phase, L = low temperature phase.

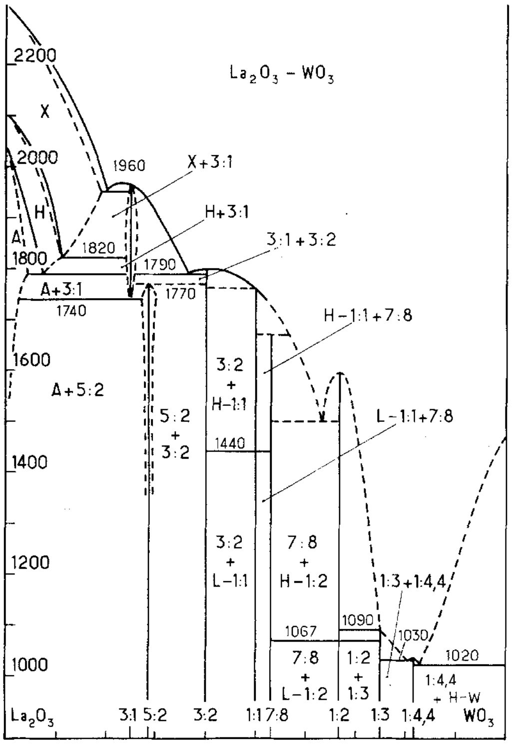

Figure 1 Phase diagram of the system La_2O_3–WO_3 [7]. The temperatures given are accurate to within ± 30° C for temperatures above 1400° C and ± 10° C for those below 1400° C. The 3:2 compound appears to have two reversible transition points at 629° C and 929° C [7], respectively. Pure WO_3 shows the following phase transition: monoclinic $\xleftrightarrow{330^\circ C}$ orthorhombic $\xleftrightarrow{740^\circ C}$ tetragonal. H – W = tetragonal WO_3, $5:2 = 5La_2O_3 \cdot 2WO_3$ solid solution, H = H-type La_2O_3 solid solution, X = X-type La_2O_3 solid solution. The others are identical to those given in the footnote of Table I.

tation of A-La_2O_3 by prolonged annealing [11]. The latter appeared to have an incongruent melting point.

The colour of glass phase ranged from colourless to pale green. Differential thermal analysis for the glass of composition 18.2% La_2O_3 showed an exothermic peak at 580° C, indicating crystallization of $La_{10}W_{22}O_{81}$ [12].

Recently, different approaches [13–15] to glass formation have been attempted by essentially employing an estimation of the critical cooling rate. The most important factor in determining the critical cooling rate appears to be the viscosity of the melts and the rising viscosity just below the solidification temperature, as pointed out by Uhlmann [16]. It is interesting to note that a glass phase was obtained for pure $La_2O_3.3WO_3$, which has a crystal structure consisting of isolated $[WO_4]$ tetrahedra [17]. No data are available for the viscosity of the melts in the La_2O_3–WO_3 system, but perhaps the melts containing isolated $[WO_4]$ polyhedra would have a lower viscosity than those containing chains or a three-dimensional network of tungstate polyhedra. The tungsten oxide, WO_3, has the structure of polymerized $[WO_6]$ octahedra, such as $[WO_6]_\infty$ [17]. A three-dimensional network is assumed in $La_{10}W_{22}O_{84}$ [12]. The compounds $La_2O_3 \cdot 2WO_3$ and $La_2O_3 \cdot WO_3$ supposedly have polymerized polyhedra from their densities, 7.5 and 7.1 g cm^{-3}, respectively. They are comparable to those of WO_3, 7.23 g cm^{-3} and $La_{10}W_{22}O_{81}$, 7.10 g cm^{-3}, and much heavier that 6.63 g cm^{-3} for $La_2O_3 \cdot 3WO_3$. Zig-zag chains of $[W_2O_9]$ have been found in $Pr_2O_3 \cdot 2WO_3$ [18]. Unfortunately, $La_2O_3 \cdot 2WO_3$ and $La_2O_3 \cdot WO_3$ have structures exceptionally different to all other $R_2O_3 \cdot 2WO_3$ and $R_2O_3 \cdot WO_3$ compounds. Their structures have not yet been determined at low temperature, but at high temperatures they have the same structure as $R_2O_3 \cdot 2WO_3$ and $R_2O_3 \cdot WO_3$ [6, 7].

According to our results shown in Table I, those reported by Topol *et al.* [2] are extremely difficult to understand in terms of the cooling rate, since no information on the latter was given. However, their method – free-fall cooling of molten spheres with hundreds of micron diameters after laser-spin melting – might have cooling rates rather slower than ours. This may imply that glass formation is also affected by other factors, such as the mechanical stress by contact with metal walls.

Acknowledgements

The authors are thankful to Drs A. Revcolevschi, A. Rouanet, and F. Sibieude for their helpful discussions.

References

1. P. T. SARJEANT and R. ROY, *J. Amer. Ceram. Soc.* **50** (1968) 500.
2. L. E. TOPOL, D. H. HENGSTENBERG, M. BLANDER, R. A. HAPPE, N. L. RICHARDSON, and L. S. NELSON, *J. Non-Cryst. Solids* **12** (1973) 377.
3. T. SUZUKI and A. M. ANTHONY, *Mat. Res. Bull.* **9** (1974) 745.

4. S. YAJIMA, K. OKAMURA, and T. SHISHIDO, *Chem. Letters, Chem. Soc, Jap.* (1973) 1327.
5. J. COUTURES, F. SIBIEUDE, A. ROUANET, M. FOEX, A. REVCOLEVSCHI, and R. COLLONGUES, *Rev. Int. Htes. Temp. et Refract.* **11** (1974) 263.
6. M. YOSHIMURA, F. SIBIEUDE, A. ROUANET and M. FOEX, *ibid* **12** (1975) 215.
7. M. YOSHIMURA and A. ROUANET, *Mat. Res. Bull.* **11** (1976) 156.
8. M. FOEX, F. SIBIEUDE, A. ROUANET, and D. HERNANDEZ, *J. Mater. Sci.* **10** (1975) 1255.
9. A. REVCOLEVSCHI, *ibid* **11** (1976) 563.
10. A. REVCOLEVSCHI, A. ROUANET, F. SIBIEUDE, and T. SUZUKI, *High temp.-High Press.* 7 (1975) 209.
11. M. YOSHIMURA, A. ROUANET, and F. SIBIEUDE, *ibid* 7 (1975) 227.
12. M. YOSHIMURA, H. MORIKAWA, and M. MIYAKE, *Mat. Res. Bull.* **10** (1975) 1221.
13. P. T. SARJEANT and R. ROY, *ibid* **3** (1968) 265.
14. J. C. A. VREESWIJK, R. G. GOSSIK, and J. M. STEVELS, *J. Non-Cryst. Solids* **16** (1974) 15.
15. T. SUZUKI and S. SAITO, *Mat. Res. Bull.* **11** (1976) 221.
16. D. R. UHLMANN, *J. Non-Cryst. Solids* 7 (1972) 337.
17. K. NASSAU and J. W. SHIEVER, NBS Special Publication No. 364, Solid State Chemistry (1972) p. 445.
18. S. V. BORISOV and R. F. KLEVTSOVA, *Kristallografiya* **15** (1970) 38, *English Trans.* **15** (1970) 28.

Received 5 August
and accepted 31 August 1976

M. YOSHIMURA
Research Laboratory of Engineering Materials,
Tokyo Institute of Technology,
Ookayama, Meguro,
Tokyo, 152,
Japan
J. COUTURES
M. FOEX
Laboratoire des Ultra-Réfractaires du C.N.R.S.,
B.P.-5 Odeillo,
66120 Font Romeu,
France

The blue chromophore in sulphur-doped borate glasses (boro-ultramarine)

Paul *et al.* [1] have recently attributed the blue colour of sulphur-doped borate glasses to the S_2^- ion. That assignment is erroneous and I will establish here that the correct identity of the species is S_3^-, the trisulphur radical anion, and point out that the authors should have considered this possibility. I will also comment on their proposed mechanism of formation of polysulphur radical anions from elemental sulphur in borate glasses.

An interest in the fascinating and ubiquitous blue chromophore formed by sulphur in a wide variety of basic or reducing media [2] brought the paper under consideration to my attention. Although the manuscript was submitted in December 1973, the literature review of the controversy concerning the identity of the blue species considered references only up to 1970, and several important studies prior to 1970 were omitted.

Paul *et al.* correctly stated that Giggenbach [3] assigned the blue species to the S_2^- ion on the basis of spectroscopic and magnetic measurements of solutions of alkali polysulphides in dimethylformamide (DMF), but they mistakenly reported that Merritt and Sawyer [4] came to the same conclusion from their studies of the electrochemical reduction of elemental sulphur in dimethyl sulphoxide. In fact, these authors first attributed the blue species to the S_8^- ion, but on re-investigation [5], which revealed an error in the coulometer reading, they concurred with the assignment of S_3^- to the blue species, suggested by other workers (*vide infra*). Although Paul *et al.* discuss the blue colour of sulphur-doped alkali halides they omit reference to the important paper by Holzer *et al.* [6]. In 1969, these authors were able to assign visible absorption bands at 400 and 610 nm to S_2^- and S_3^-, respectively, by an elegant application of Raman spectroscopy. During the period 1970–73, the blue colour of (a) ultramarine [7, 8], (b) sulphur solutions in an LiCl–KCl eutectic [9], (c) solutions of alkali polysulphides in hexamethylphosphoramide [10] or DMF [11, 12] was attributed to the S_3^- ion. French workers [13], who studied the electrochemical reduction of elemental sulphur at an inert electrode in DMF or DMSO, originally proposed S_6^{2-} for the blue species, but in a full account of their work published recently [14], they agree with the assignment of S_3^-. Thus in